PRESSURE TREATMENT OF METALS / ОБРАБОТКА МЕТАЛЛОВ ДАВЛЕНИЕМ

UDC 620.172.2.087.45
https://doi.org/10.17073/0021-3438-2023-3-79-88

Research article
Научная статья

Using the method of correlation of digital images for plotting stress–strain curves in true coordinates

A.D. Monakhov[1], M.M. Gulyaev[2], N.E. Gladysheva[2], O.Yu. Kopteltseva[2], V.V. Avtaev[1], N.O. Yakovlev[1], I.V. Gulina[1]

[1] **All-Russian Research Institute of Aviation Materials of the National Research Center "Kurchatov Institute"**
17 Radio str., Moscow, 105005, Russia

[2] **Joint Stock Company "Design Bureau of Instrument Engineering named after Academician A.G. Shipunov"**
59 Shcheglovskaya Zaseka str., Tula, 300004, Russia

✉ Anton D. Monakhov (ant.monakhov@gmail.com)

Abstract: This article describes the features of determining strain curves in true stress–true strain coordinates, using samples of circular cross section from Al–Cu–Mg–Zn aluminum alloy. The calculation and experimental methods of determining true stresses and strains were compared. Calculation methods based on the condition of volume constancy may not reflect actual regularities of deformation at the stage of strain localization in the considered material. Nevertheless, the use of systems of digital image correlation (DIC) allows measurements of both the geometrical sizes of deformed sample and strain fields on its surface to be performed, including on the sample neck. It was demonstrated that the measurement error of the sample diameter by the coordinate field was 0.02 mm at the instance of destruction. In order to improve the measurement precision, an increase in the recording frequency in proportion to increase in strain rate was proposed, as well as measuring the surface coordinates from both sides of the sample. It is also possible to supplement the strain curves obtained by DIC optical systems with the measurements of true fracture stress, and the true fracture strain determined by calculations on the destructed sample. The presented methods of analysis of plastic flow by direct measurement of field displacements and strains allow actual regularities between true stresses and strains at the interval of irregular plastic strain to be established. This cannot be achieved by analytical conversion of conventional curve. The obtained hardening coefficients and strain curves can be used for simulation and design of machinery structures and parts.

Keywords: true stress, true strain, plastic strain, strain field, correlation of digital images, strain hardening.

For citation: Monakhov A.D., Gulyaev M.M., Gladysheva N.E., Kopteltseva O.Yu., Avtaev V.V., Yakovlev N.O., Gulina I.V. Using the method of correlation of digital images for plotting stress–strain curves in true coordinates. *Izvestiya. Non-Ferrous Metallurgy.* 2023;29(3):79–88. https://doi.org/10.17073/0021-3438-2023-3-79-88

Применение метода корреляции цифровых изображений для построения диаграмм деформирования в истинных координатах

А.Д. Монахов[1], М.М. Гуляев[2], Н.Е. Гладышева[2], О.Ю. Коптельцева[2], В.В. Автаев[1], Н.О. Яковлев[1], И.В. Гулина[1]

[1] **Всероссийский научно-исследовательский институт авиационных материалов Национального исследовательского центра «Курчатовский институт»**
105005, Россия, г. Москва, ул. Радио, 17

[2] **АО «Конструкторское бюро приборостроения им. академика А.Г. Шипунова»**
300004, Россия, г. Тула, ул. Щегловская Засека, 59

✉ Антон Дмитриевич Монахов (ant.monakhov@gmail.com)

Аннотация: Приведены особенности определения диаграмм деформирования в координатах «истинное напряжение – истинная деформация» на образцах круглого сечения из алюминиевого сплава системы Al–Cu–Mg–Zn. Выполнено сравнение расчетных и экспериментальных методов определения истинных напряжений и деформаций. Расчетные методы, основанные на применении условия постоянства объема, могут не отражать действительных закономерностей деформирования на этапе локализации деформации в материале исследуемого образца, в то время как использование систем корреляции цифровых изображений (КЦИ) позволяет проводить измерения как геометрических размеров деформируемого образца, так и полей деформаций на его поверхности, в том числе непосредственно в шейке образца. Показано, что ошибка измерения диаметра образца по полю координат в момент разрушения составила 0,02 мм. С целью повышения точности измерения предложено увеличение частоты съемки пропорционально возрастанию скорости деформирования, а также проведение измерения координат поверхности с двух сторон образца. Также возможно дополнять полученные с помощью оптических систем КЦИ кривые деформирования результатами измерения истинного разрушающего напряжения и истинной разрушающей деформацией, определенными расчетным способом по разрушенному образцу. Представленные способы исследования пластического течения материала непосредственным измерением полей перемещений и деформаций позволяют устанавливать действительные закономерности между истинными напряжениями и деформациями на участке неравномерного пластического деформирования, чего достичь аналитическим пересчетом условной диаграммы невозможно. Полученные коэффициенты упрочения и кривые деформирования могут быть использованы при моделировании и проектировании конструкций и деталей машин.

Ключевые слова: истинное напряжение, истинная деформация, пластическая деформация, поле деформации, корреляция цифровых изображений, деформационное упрочнение.

Для цитирования: Монахов А.Д., Гуляев М.М., Гладышева Н.Е., Коптельцева О.Ю., Автаев В.В., Яковлев Н.О., Гулина И.В. Применение метода корреляции цифровых изображений для построения диаграмм деформирования в истинных координатах. *Известия вузов. Цветная металлургия*. 2023;29(3):79–88.
https://doi.org/10.17073/0021-3438-2023-3-79-88

Introduction

Machinery structures and parts should be designed with consideration for provision of their safe operation. Permissible operation stresses are determined by criteria of ultimate stress state [1; 2]. This in their turn are compared with the results obtained upon uniaxial strain [3—6]. Standard tension or compression state allow strain curve in stress—strain coordinates to be established (curve *1* in Fig. 1) [7]. Stress strain curves can also be referred to as conditional, since the surface area of transversal cross section and strain measurement base are assumed to be constant throughput the test. In order to establish true regularities between stress and strain [8], as well as during simulation of plasticity problems by finite element method [9; 10], true stresses and true strains (curve *2* in Fig. 1) need to be applied in operations. These are calculated by correlating the load and the absolute elongation of the sample to the actual area of true surface area of transversal cross section and the length of working part, respectively.

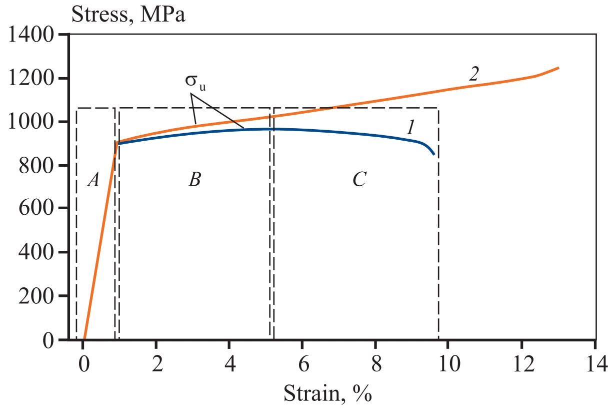

Fig. 1. Conditional (*1*) and true (*2*) strain curves

Рис. 1. Условная (*1*) и истинная (*2*) диаграммы деформирования

The development of computation devices has allowed the regularities of material flow to be studied not only by analytical methods [8; 11], but also by direct measurements of displacements, strains or geometry of the object in the region of local stability loss. This work considers the use of optical contactless tensometry systems in determining strain curves in true coordinates. The calculations of true stresses by analytical and experimental methods of direct recording of strain and surface area of transversal cross section in the region of plastic flow were compared for isotropic materials.

Calculation method of determination of strain curves in true coordinates

Three characteristic segments in conditional strain curve of plastic material can be highlighted. The segment of elastic plastic strain (region *A* in Fig. 1) is characterized by an insignificant difference in the conditional and true curves due to moderate strains. The hardening segment (region *B* in Fig. 1) is characterized by a monotonous increase in stress both in true and in conditional coordinates, due to a the limitation of ultimate strength (σ_u). In the segment of localization of plastic strain (region *C* in Fig. 1) neck formation can be observed. This can be seen in the transfer from uniform strain, acting along the entire length of working part, to a localized one resulting in load drop upon strain growth. The region of neck formation is also characterized by the transfer from a uniaxial (simple) stressed state to complex stress strain state. This exerts significant influence on strain [12; 13].

Using the calculation method, the surface area of transversal cross section during test for the segments of elastic plastic strain and hardening can be determined from the condition of volume constancy [11]:

$$F_0 dz = F(1 + \varepsilon)dz, \quad (1)$$

where F_0 is the surface area of transversal cross section at initial test time; F is the surface area of transversal cross section during strain; ε is the relative strain; dz is the absolute change of length during strain.

The surface area of transversal cross section can be expressed using Eq. (1):

$$F = F_0/(1 + \varepsilon). \quad (2)$$

True stresses upon uniform strain equal to the ratio of load upon strain to the surface area of transversal cross section can be determined by Eq. (2):

$$s = P/F = \sigma(1 + \varepsilon), \quad (3)$$

where s is the true stress; P is the load during strain; σ is the conditional stress.

True strains can be determined as the ratio of absolute elongation to total length of canulated zone [11]:

$$\varphi = \int_{l_0}^{l} dl/l = \ln(l/l_0) = \ln(1 + \varepsilon), \quad (4)$$

where φ is the true strain; l is the total length of calculated zone; l_0 is the initial length of working zone.

The strain curve in true coordinates for uniform strain is plotted by Eqs. (3), (4). True fracture strain and true fracture stress are applied to the strain curve and calculated as follows [11; 12]:

$$s_f = \sigma_r / (1 - \psi), \quad (5)$$

where s_f are the true fracture stresses; σ_r are the conditional stresses upon rupture; ψ is the relative reduction of area after rupture;

$$\varphi_f = \ln(1 - \psi)^{-1}, \quad (6)$$

where φ_f is the true fracture strain.

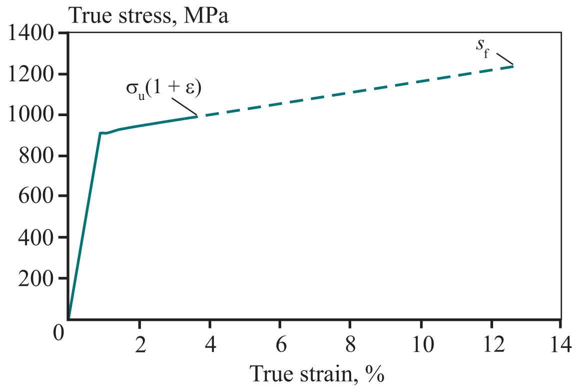

Fig. 2. Schematic strain curve in true coordinates obtained by calculations

Рис. 2. Схематичная диаграмма деформирования в истинных координатах, полученная расчетным способом

The calculation method of plotting strain curves in true coordinates (Fig. 2) does not require special equipment, and can be characterized by its simplicity. However, the curve may not reflect actual regularities of strain at the segment of localization of plastic strain. This method is recommended for brittle materials.

Determining strain curves in true coordinates using strain fields

Observation of the fields of strains and displacements allows the true stresses and strains for all strain segments to be calculated. Several methods are available to determine the fields of strains and displacements [14; 15]. For reasons of precision [16] and simplicity, the method of digital image correlation (DIC) was selected.

The DIC method is based on video recording the sample during the test and alternate comparison of frames before and after strain, The aim was to determine displacements of uniformly subdivided field segments (subregions). A chaotic spotted structure (speckle pattern) is applied beforehand onto a sample so that each sub-region differs from the others. The fields of displacements and strains are calculated using the displacement of sub-regions. Two cameras allow the position of points to be determined and their displacement in three coordinates to be calculated.

The DIC systems allow local strain fields to be formed over the entire analyzed surface, including the neck zone, while extensometers perform measurements between two predefined points. Thus, the strain determined by extensometers at the segment of neck formation is the arithmetic mean between localized and uniform plastic strain according to measurements. A uniform or localized deformation cannot be distinguished from a general deformation.

Substituting the mean arithmetic value of longitudinal strain (ε_{yy}^{max}) along the transversal section of sample neck (Fig. 3) into Eqs. (3) and (4) in place of the relative strain (ε), we can obtain equations for determining true stresses and strains along longitudinal component of strain tensor for any strain stage [17]:

$$s = \sigma(1 + \varepsilon_{yy}^{max}), \quad (7)$$

$$\varphi = \ln(1 + \varepsilon_{yy}^{max}). \quad (8)$$

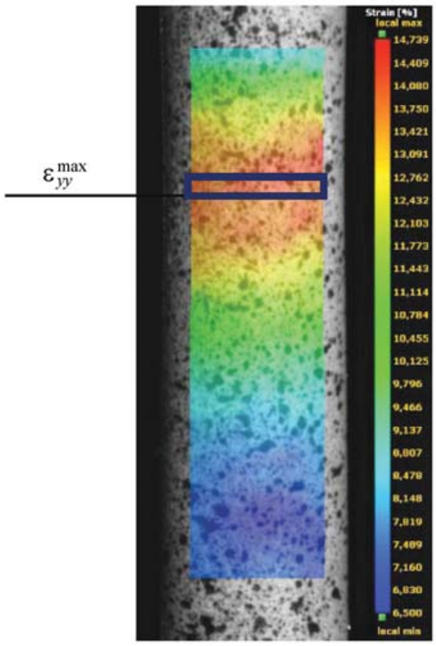

Fig. 3. Field of longitudinal component of strain tensor ε_{yy}

Рис. 3. Поле продольной компоненты тензора деформации ε_{yy}

This method allows analysis at all strain stages to be performed. However, Eqs. (7) and (8) were derived assuming the volume constancy for isotropic materials. Therefore, the possibility of applying these interrelations for orthotropic and anisotropic materials should be studied in more detail.

When observing the positions of sub-regions in the calculation of the fields of displacements and strains, the sample diameter at any time of tests along the entire length of the considered region can be measured. A circle was inscribed using the least square method into the coordinates of transversal section in the plane of the maximum reduction of sample area. The sample diameter in the course of strain was determined by Eq. (9):

$$d_i = 2[(x - a)^2 + (y - b)^2]^{1/2}, \quad (9)$$

where x, y are the coordinates of circumference point along the respective axes; a, b are the coordinates of circumference center along the axes X, Y, respectively.

Experimental

Strain curves in true coordinates were determined on a sample of circle cross section from aluminum alloy Al—Cu—Mg—Zn. The sample diameter was 5.92 mm, and the length of working part: 30 mm. The tests were carried out using an electromechanical test machine with a rated load of 100 kN at constant speed of active clamp, equal to 2 mm/min. Throughout the test, the longitudinal strain (ε) was recorded using a contactless extensometer. The strain fields were determined using a DIC system comprising of two cameras with a resolution of 3 megapixels, providing a pixel density of 31 dot/mm. The subregion step was 8 dots, and the subregion size: 25×25 dots. The recording frequency was 5 Hz. The physicomechanical properties determined by conditional strain curve (Fig. 4) are summarized in Table 1, the relative elongation (δ_5) and the relative reduction of area (ψ) were determined in accordance with the State standard GOST 1497-84.

In Fig. 5, numbers *1* and *2* denote the coordinates of points of section in initial state and preceding the sample destruction, respectively. The diameter of inscribed circle for a sample before strain (line *1* in Fig. 5) was equal to 5.92 mm, and for a sample before destruction (*2* in Fig. 5) to 5.24 mm.

The actual sample diameter after rupture was assumed to be higher than that measured along inscribed circle by the elastic constituent of ε_{xx}. It was also assumed to be equal to 5.25 mm, since during measuring of diameter the sample was still in stressed state. However, the actual sample diameter after rup-

Table 1. **Physicomechanical properties**

Таблица 1. Физико-механические характеристики исследуемого образца

Poisson ratio μ	Elasticity modulus E, GPa	Yield stress $\sigma_{0,2}$, MPa	Ultimate tensile strength σ_u, MPa	Rupture stress σ_r, MPa	Relative elongation δ_5, %	Relative reduction of area ψ, %
0.32	72	600	640	593	10.0	20.0

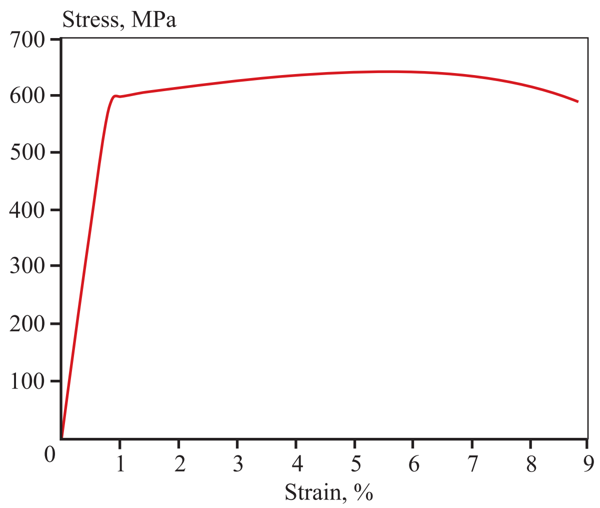

Fig. 4. Strain curve in conditional coordinates

Рис. 4. Диаграмма деформирования в условных координатах

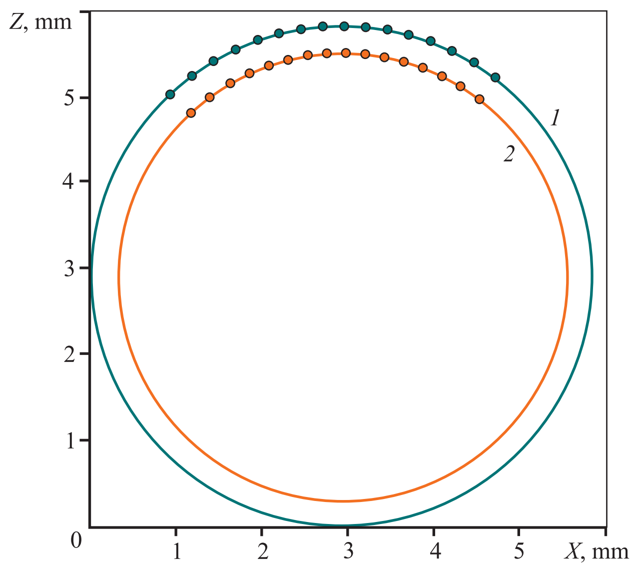

Fig. 5. Diameter measurement by inscribed circle

Рис. 5. Измерение диаметра образца по вписанной окружности

ture was lower than that measured along the inscribed circle and was equal to 5.23 mm. This can be attributed to the fact that the test was carried out at a constant active clamp speed and constant recording frequency. Thus, as a consequence of strain localization the strain rate was increased from 0.0002 s^{-1} at the elastic segment to 0.018 s^{-1} at the instance preceding destruction. Thus, Fig. 6 illustrated true strain as a function of test time (curve *1*) and its derivative of time: strain rate (curve *2*) for segments of elastic plastic strain (*A*), hardening (*B*) and localization of plastic flow (*C*). Respectively, the recording at the frequency of 5 Hz allowed true strain to be resolved with a precision of 0.0036 m/m per frame at the instance preceding destruction.

The true stresses were calculated using the determined diameters:

$$S = P/F = 4P/(\pi d_i^2), \quad (10)$$

where P is the load during strain, d_i is the sample diameter during strain.

As a consequence of complicated and heterogeneous stress strain state, occurring in the region of strain localization [12; 13], the strain can be heterogeneous. Therefore, the profile of transversal cross section will differ from a circle. In order to account for eccentricity when calculating the surface area of transversal cross section during strain, it is recommended that the fields of displacement and strain on two opposite sides be studied by four cameras calibrated as a single system [18].

Based on test results, the strain curves in true coordinates were plotted Fig. 7 shows Curve *1*, based on calculations, curve segment (dashed line), linearly interpolated up to the points determined by Eqs. (5), (6), as well as Curve *2*, plotted on the basis of longitudinal Lagrange strain, ε_{yy}, as well as curve *3*, calculated by actual change in diameter during strain.

The elastic segments of loading in the strain curves in true coordinates coincide for all calculation methods. Differences are observed in the hardening segment.

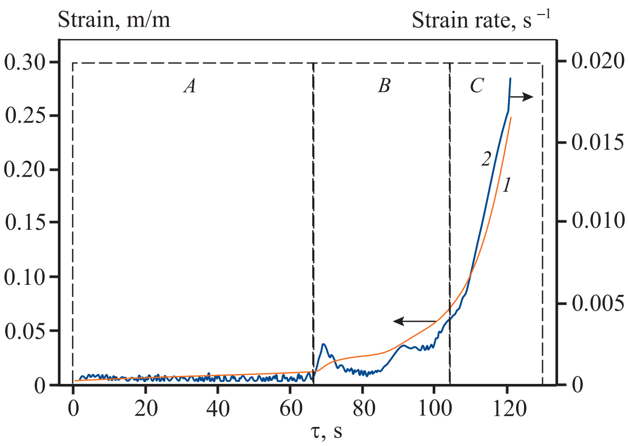

Fig. 6. Relative strain as a function of test duration

Рис. 6. Диаграмма зависимости относительной деформации от времени испытания

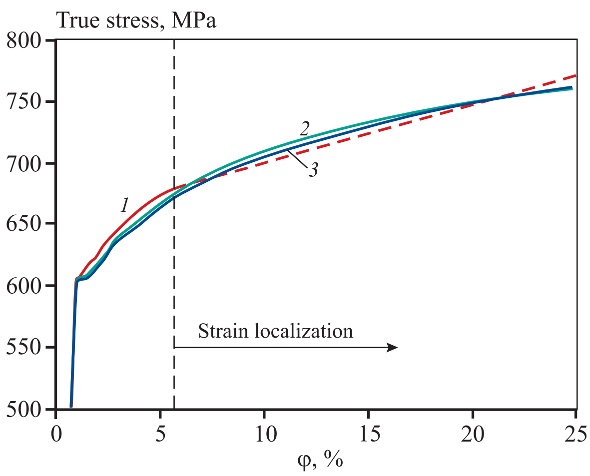

Fig. 7. Strain curves in in true coordinates

Рис. 7. Диаграммы деформирования в истинных координатах

The most common and simplest approximation method of plastic behavior is the strain hardening exponent [19—21], Its coefficients can be also used to describe strain hardening of material in the course of finite element simulation:

$$S = Kp^n, \qquad (11)$$

where K is the strength coefficient determined by the least square method, MPa; n is the coefficient of strain hardening determined by the least square method; p is the true plastic strain; S is the true stress, MPa.

Figure 8 illustrates the hardening segments in true stress—true plastic strain coordinates for strain curves in true coordinates. This is obtained by calculations (Fig. 8, *a*): by the field of longitudinal strains in the region of strain localization (Fig. 8, *b*), as well as calculating the sample diameter by means of an inscribed circle in the coordinates of points of the highest longitudinal strains (Fig. 8, *c*). The dashed line in Fig. 8 shows their exponential model of approximation obtained by the least square method on the basis of data of logarithmically linearized hardening curve. The calculated results are summarized in Table 2.

The approximation model was determined for the hardening segment obtained by means of calculation, but only to ultimate strength. This indicates that it cannot be used for strains exceeding the ultimate strength. At the same time, the methods based on DIC systems allow true stresses to be determined as a function of true strain up to sample destruction. However, for the more uniform control of strain in the sample neck by optical system, the test machine needs to be controlled by true strains or for the recoding frequency of DIC system to be increased in proportion to strain rate. Otherwise, the strain curves obtained by DIC systems must be supplemented by true fracture stress and

Table 2. **Calculations of strain curves in true coordinates**

Таблица 2. Результаты расчетов диаграмм деформирования в истинных координатах

Method of determination	K, MPa	n	True fracture stress (S_f), MPa	True fracture strain (φ_f), %
Calculations	792	0.0518	771	25.1
By longitudinal component of strain tensor	834	0.0685	761	24.9
By change in diameter	831	0.0687	762	24.9

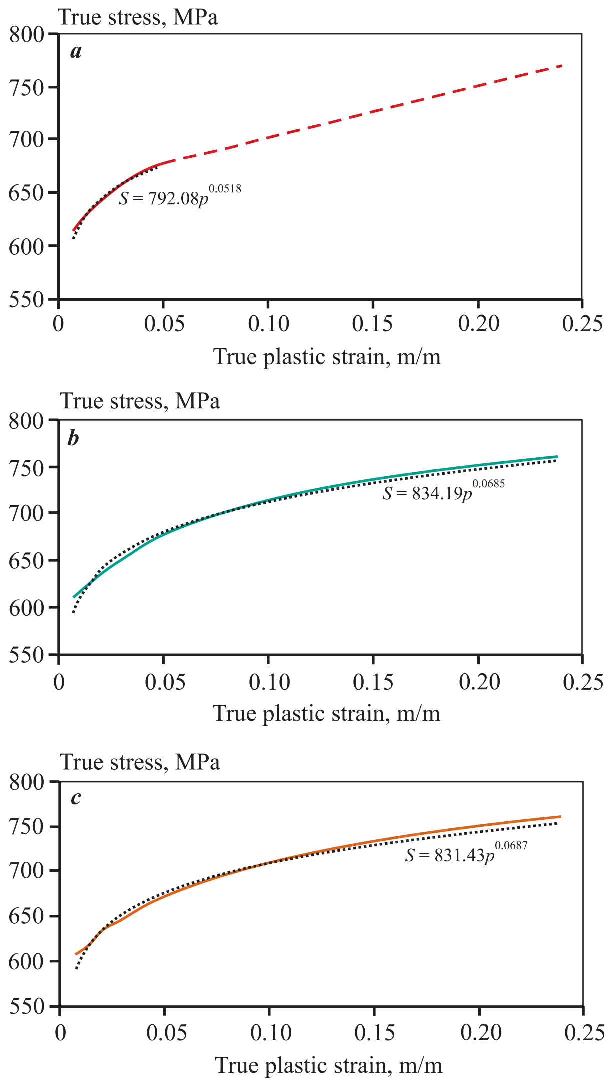

Fig. 8. Hardening segments of strain curves in true coordinates obtained by calculations (***a***), by field of longitudinal strain in sample neck (***b***) and by change in diameter (***c***)

Рис. 8. Участки упрочнения диаграмм деформирования в истинных координатах, полученные расчетным методом (***a***), по полю продольных деформаций в шейке образца (***b***) и по изменению диаметра образца (***c***)

true fracture strain determined by calculations using destructed sample.

Conclusions

The strain curves in true coordinates provide data on the strain hardening of material and can be used in the simulation and design of parts and structures [9; 22].

The research methods of plastic flow by direct measurement of fields of displacement and strain allow actual regularities between true stresses and strains at the interval of irregular plastic strain to be established. This cannot be achieved by the analytical conversion of a conventional curve. In addition, it should be taken into account that after neck formation, the strain rate increases. This results in additional errors in the calculation of true stresses and strains, which at the instance of sample destruction can reach 1.3 % with respect to the values obtained by actual measurement of sample after destruction. However, the calculation method of curve determination in true coordinates is simple. It does not require additional hard- or software. True fracture stress and true strain upon breakage determined by means of this method can supplement the results of actual measurements.

The selection of calculation methods of strain curves in true coordinates is stipulated by the requirement for the completeness of results, as well as the material type. It should also be mentioned that both methods based on the use of DIC systems provide equal amount of data, and the difference between the results obtained in this work can be neglected (the difference between true fracture stresses is less than 0.2 %). However, the use of the longitudinal component of strain tensor upon analysis of anisotropic material can lead to calculation errors. Therefore, the preferred method is based on measurement of actual sample diameter in the course of deformation by using DIC systems on two sides.

References

1. Oreshko E.I., Erasov V.S., Grinevich D.V., Shershak P.V. Review of criteria of durability of materials. *Trudy VIAM*. 2019;(9(81)):108—126. (In Russ.).
https://doi.org/10.18577/2307-6046-2019-0-9-108-126
Орешко Е.И., Ерасов В.С., Гриневич Д.В., Шершак П.В. Обзор критериев прочности материалов. *Труды ВИАМ*. 2019;(9(81)):108—126.
2. Yakovlev N.O., Grinevich D.V., Mazalov P.B. Mathematical simulation of the stress-strain state manifesting during compression of a lattice structure manufactured by means of selective laser melting. *Vestnik Moskovskogo gosudarstvennogo tekhnicheskogo universiteta im. N.E. Baumana. Seriya Estestvennye nauki*. 2018;(6(81)):113—127. (In Russ.).
https://doi.org/10.18698/1812-3368-2018-6-113-127
Яковлев Н.О., Гриневич Д.В., Мазалов П.Б. Математическое моделирование напряженно-де-

формированного состояния при сжатии сетчатой конструкции, синтезированной методом селективного лазерного сплавления. *Вестник Московского государственного технического университета им. Н.Э. Баумана. Серия Естественные науки*. 2018;(6(81)): 113—127.
3. Kablov E.N., Podzhivotov N.Yu., Lutsenko A.N. About need for creation of uniform information and analysis centerof aviation materials of the Russian Federation. *Problemy mashinostroeniya i avtomatizatsii*. 2019;(3): 28—34. (In Russ.).
Каблов Е.Н., Подживотов Н.Ю., Луценко А.Н. О необходимости создания единого информационно-аналитического центра авиационных материалов РФ. *Проблемы машиностроения и автоматизации*. 2019;(3):28—34.
4. Grinevich A.V., Slavin A.V., Yakovlev N.O., Monakhov A.D., Gulina I.V. On problem of spalling fracture of high-strength steel under quasi-static tension. *Deformatsiya i razrushenie materialov*. 2021;(8):2—7. (In Russ.).
https://doi.org/10.31044/1814-4632-2021-8-2-7
Гриневич А.В., Славин А.В., Яковлев Н.О., Монахов А.Д., Гулина И.В. К вопросу откольного разрушения высокопрочной стали при квазистатическом растяжении. *Деформация и разрушение материалов*. 2021;(8): 2—7.
5. Kablov E.N. Formation of domestic space materials science. *Vestnik RFFI*. 2017;(3):97—105. (In Russ.).
https://doi.org/10.22204/2410-4639-2017-095-03-97-105
Каблов Е.Н. Становление отечественного космического материаловедения. *Вестник РФФИ*. 2017;(3):97—105.
6. Dowling N. Mechanical behavior of materials: Engineering methods for deformation, fracture and fatigue. 4 ed. Essex: Pearson, 2013. 977 p.
7. Oreshko E.I., Erasov V.S., Krylov V.D. Construction of 3d stress-strain diagram for the analysis of mechanical behavior of the material tested at various loading rates. *Aviatsionnye materialy i tekhnologii*. 2018;(2(51)):59—66. (In Russ.).
https://doi.org/10.18577/2071-9140-2018-0-2-59-66
Орешко Е.И., Ерасов В.С., Крылов В.Д. Построение трехмерных диаграмм деформирования для анализа механического поведения материала, испытанного при различных скоростях нагружения. *Авиационные материалы и технологии*. 2018;(2(51)):59—66.
8. Kachanov L.M. Fundamentals of fracture mechanics. Moscow: Nauka, 1974. 311 p. (In Russ.).
Качанов Л.М. Основы механики разрушения. М.: Наука, 1974. 311 с.
9. Petrík A., Ároch R. Usage of true stress-strain curve for FE simulation and the influencing parameters. *IOP Conference Series: Materials Science and Engineering*. 2019;566:012025.
http://dx.doi.org/10.1088/1757-899X/566/1/012025
10. Terhorst M., Ozhoga-Maslovskaja O., Trauth D., Mattfeld P., Klocke F. Finite element-based modeling of strain hardening in metal forming. *Steel Research International*. 2016;87(10):1323—1332.
https://doi.org/10.1002/srin.201500375
11. Birger I.A., Mavlyutov R.R. Strength of materials. Moscow: Nauka, 1986. 561 p. (In Russ.).
Биргер И.А., Мавлютов Р.Р. Сопротивление материалов. М.: Наука, 1986. 561 с.
12. Osintsev A.V., Plotnikov A.S., Morozov E.M., Lubkova E.Yu. On the location of a neck formation during the tension of cylindrical specimens. *Letters on Materials*. 2017;7(3):260—265.
https://doi.org/10.22226/2410-3535-2017-3-260-265
13. Junfu Chen, Zhiping Guan, Pinkui Ma, Zhigang Li, Xiangrui Meng. The improvement of stress correction in post-necking tension of cylindrical specimen. *The Journal of Strain Analysis for Engineering Design*. 2019;54(3): 209—222.
http://dx.doi.org/10.1177/0309324719852875
14. Monakhov A.D., Yakovlev N.O., Avtaev V.V., Kotova E.A. Destructive methods for determining residual stresses (review). *Trudy VIAM*. 2021;(9(103)):95—104. (In Russ.).
http://dx.doi.org/10.18577/2307-6046-2021-0-9-95-104
Монахов А.Д., Яковлев Н.О., Автаев В.В., Котова Е.А. Разрушающие методы определения остаточных напряжений (обзор). *Труды ВИАМ*. 2021;(9(103)): 95—104.
15. Huang L., Korhonen R.K., Turunen M.J., Finnilä M.A.J. Experimental mechanical strain measurement of tissues. *Peer J*. 2019;7:e6545.
https://doi.org/10.7717%2Fpeerj.6545
16. Sutton M.A., Orteu J.-J., Schreier H.W. Image correlation for shape, motion and deformation measurements. Columbia, SC, USA: University of South Carolina, 2009. 322 p.
17. Yang L., Smith L. Measure strain distribution using digital image correlation (DIC) for tensile tests. Final Report. Auto/Steel Partnership. 2010. 26 p.
18. Junrui L., Guobiao Y., Thorsten S. A method of the direct measurement of the true stress—strain curve over a large

strain range using multi-camera digital image correlation. *Optics and Lasers in Engineering*. 2018;(107):194—201. https://doi.org/10.1016/j.optlaseng.2018.03.029

19. Shchetinina N.D., Rudchenko A.S., Selivanov A.A. The approaches that are used for developed of optimal strain modes of aluminum-lithium alloys (review). *Trudy VIAM*. 2019;(8(90)):20—34. (In Russ.). https://doi.org/10.18577/2307-6046-2020-0-8-20-34
Щетинина Н.Д., Рудченко А.С., Селиванов А.А. Применение методов математического моделирования при разработке режимов деформации алюминий-литиевых сплавов (обзор). *Труды ВИАМ*. 2019;(8(90)):20—34.
20. Poole W.J., Embury J.D., Lloyd D.J. Work hardening in aluminium alloys. In: *Fundamentals of aluminium metallurgy*. Ed. Roger Lumley. Woodhead Publishing Limited, 2011. P. 307—344. https://doi.org/10.1533/9780857090256.2.307
21. Den Uijl N.J., Carless L.J. Advanced metal-forming technologies for automotive applications. In: *Advanced materials in Automotive Engineering*. Ed. Jason Rowe. Woodhead Publishing Limited, 2012. P. 28—56. https://doi.org/10.1533/9780857095466.28
22. Faridmehr I., Osman M.H., Adnan A.B., Nejad A.F., Hodjati R., Azimi M. Correlation between engineering stress-strain and true stress-strain curve. *American Journal of Civil Engineering and Architecture*. 2014;2(1):53—59. http://dx.doi.org/10.12691/ajcea-2-1-6

Information about the authors

Anton D. Monakhov – Engineer of the Laboratory of Strength and Reliability of Aircraft Materials, All-Russian Research Institute of Aviation Materials (VIAM) of the National Research Center (NRC) “Kurchatov Institute”.
https://orcid.org/0000-0002-8249-5814
E-mail: ant.monakhov@gmail.com

Maksim M. Gulyaev – Head of the Department of the Joint Stock Company (JSC) “Design Bureau of Instrument Engineering (KBP) named after Academician A.G. Shipunov”.
https://orcid.org/0000-0003-0058-4694
E-mail: guliaevmay@mail.ru

Natalya E. Gladysheva – Head of the Sector of the JSC “KBP named after Academician A.G. Shipunov”.
https://orcid.org/0000-0001-9423-1683
E-mail: naeglad@mail.ru

Olga Yu. Kopteltseva – Leading Research Engineer of the JSC “KBP named after Academician A.G. Shipunov”.
https://orcid.org/0000-0002-7736-0480
E-mail: olya_moshkina@mail.ru

Vitaliy V. Avtaev – Leading Engineer of the Laboratory of Strength and Reliability of Aircraft Materials, NRC “Kurchatov Institute” – VIAM.
https://orcid.org/0000-0001-6825-0602
E-mail: darkee@mail.ru

Информация об авторах

Антон Дмитриевич Монахов – инженер лаборатории прочности и надежности материалов воздушного судна Всероссийского научно-исследовательского института авиационных материалов (ВИАМ) Национального исследовательского центра (НИЦ) «Курчатовский институт».
https://orcid.org/0000-0002-8249-5814
E-mail: ant.monakhov@gmail.com

Максим Михайлович Гуляев – начальник отдела АО «Конструкторское бюро приборостроения (КБП) им. академика А.Г. Шипунова».
https://orcid.org/0000-0003-0058-4694
E-mail: guliaevmay@mail.ru

Наталья Евгеньевна Гладышева – начальник сектора АО «КБП им. А.Г. Шипунова».
https://orcid.org/0000-0001-9423-1683
E-mail: naeglad@mail.ru

Ольга Юрьевна Коптельцева – ведущий инженер-исследователь АО «КБП им. А.Г. Шипунова».
https://orcid.org/0000-0002-7736-0480
E-mail: olya_moshkina@mail.ru

Виталий Васильевич Автаев – ведущий инженер лаборатории прочности и надежности материалов воздушного судна НИЦ «Курчатовский институт» – ВИАМ.
https://orcid.org/0000-0001-6825-0602
E-mail: darkee@mail.ru

Nikolai O. Yakovlev – Cand. Sci. (Eng.), Head of the Laboratory of Strength and Reliability of Aircraft Materials, NRC "Kurchatov Institute" – VIAM.
https://orcid.org/0000-0002-3663-8239
E-mail: nick_62@mail.ru

Irina V. Gulina – Deputy Head of the Laboratory of Strength and Reliability of Aircraft Materials, NRC "Kurchatov Institute" – VIAM.
https://orcid.org/0000-0001-5934-2249.
E-mail: iragoolina@gmail.com

Николай Олегович Яковлев – к.т.н., начальник лаборатории прочности и надежности материалов воздушного судна НИЦ «Курчатовский институт» – ВИАМ.
https://orcid.org/0000-0002-3663-8239
E-mail: nick_62@mail.ru

Ирина Владимировна Гулина – заместитель начальника лаборатории прочности и надежности материалов воздушного судна НИЦ «Курчатовский институт» – ВИАМ.
https://orcid.org/0000-0001-5934-2249
E-mail: iragoolina@gmail.com

Contribution of the authors

A.D. Monakhov – conducted experiments, conducted the calculations, processed the research results, wrote the manuscript, analyzed the research results, formulated the conclusions of the article.

M.M. Gulyaev – prepared the experiment, formulated the main concept, defined the goal and objectives of the study, revised the manuscript, revised the conclusions, provided resources.

N.E. Gladysheva – prepared the experiment, formulated the main concept, defined the goal and objectives of the study, revised the manuscript, revised the conclusions, provided resources.

O.Yu. Kopteltseva – prepared the experiment, formulated the main concept, defined the goal and objectives of the study, revised the manuscript, revised the conclusions, provided resources

V.V. Avtaev – conducted calculations, processed the research results, revised the manuscript, managed the experiment, formulated the conclusions.

N.O. Yakovlev – scientific advising, formulated the main concept, revised the manuscript, revised the conclusions.

I.V. Gulina – conducted the calculations revised the manuscript, revised the conclusions, provided resources, managed the experiment.

Вклад авторов

А.Д. Монахов – проведение экспериментов, проведение расчетов, обработка результатов исследований, подготовка текста статьи, анализ результатов исследований, формулировка выводов статьи.

М.М. Гуляев – подготовка эксперимента, формирование основной концепции, постановка цели и задачи исследования, корректировка текста статьи, корректировка выводов статьи, обеспечение ресурсами.

Н.Е. Гладышева – подготовка эксперимента, формирование основной концепции, постановка цели и задачи исследования, корректировка текста статьи, корректировка выводов статьи, обеспечение ресурсами.

О.Ю. Коптельцева – подготовка эксперимента, формирование основной концепции, постановка цели и задачи исследования, корректировка текста статьи, корректировка выводов статьи, обеспечение ресурсами.

В.В. Автаев – проведение расчетов, обработка результатов исследований, корректировка текста статьи, руководство проведением эксперимента, формулировка выводов статьи.

Н.О. Яковлев – научное руководство, формирование основной концепции, корректировка текста статьи, корректировка выводов статьи.

И.В. Гулина – проведение расчетов, корректировка текста статьи, корректировка выводов статьи, руководство проведением эксперимента.

The article was submitted 28.12.2022, revised 20.04.2023, accepted for publication 24.04.2023

Статья поступила в редакцию 28.12.2022, доработана 20.04.2023, подписана в печать 24.04.2023